European Spine Journal (2024) 33:1230–1244
https://doi.org/10.1007/s00586-023-08111-7

ORIGINAL ARTICLE

Diagnostic efficacy of tract-specific diffusion tensor imaging in cervical spondylotic myelopathy with electrophysiological examination validation

Yanming Fang[1,2] · Sisi Li[3] · Jinchao Wang[1,2] · Zhenzhen Zhang[1,4] · Wen Jiang[1,5] · Chao Wang[1,6] · Yuancheng Jiang[3] · Hua Guo[3] · Xiao Han[1,2,6] · Wei Tian[1,2]

Received: 1 May 2023 / Revised: 2 November 2023 / Accepted: 17 December 2023 / Published online: 29 January 2024

Abstract

Purpose This study aimed to investigate the effectiveness of tract-specific diffusion tensor imaging (DTI) metrics in identifying the responsible segments for neurological dysfunction in cervical spondylotic myelopathy (CSM).

Methods The study encompassed nineteen participants diagnosed with CSM, including 10 males and 9 females. Additionally, a control group consisting of ten healthy caregivers (5 males and 5 females) were recruited with no symptoms and no compressions on magnetic resonance imaging (MRI). All participants underwent a comprehensive physical examination, MRI assessment, and DTI examination conducted by a senior chief physician. Several parameters were collected from the MR images, including the aspect ratio (defined as the anteroposterior diameter / the transverse diameter of the corresponding segment's spinal cord), transverse ratio (defined as the transverse diameter of the corresponding segment's spinal cord / the transverse diameter of the spinal cord at C2/3), and T2 high signal of the spinal cord. Furthermore, quantitative DTI metrics, such as axial diffusivity (AD), mean diffusivity (MD), radial diffusivity (RD), and fractional anisotropy (FA), were calculated using automatic region-of-interest (ROI) analysis for both whole spinal cord column and dorsal column. Receiver operating characteristic (ROC) curves were constructed to evaluate the diagnostic efficacy of the aspect ratio, transverse ratio, and DTI parameters. The area under the curve (AUC), sensitivity, and specificity were calculated. Intraoperative spinal cord electrophysiological examination was performed as the objective measure of spinal cord function during surgery.

Results As determined by electrophysiological examination, neurological dysfunction was found in 2 patients due to C3/4 compression, in 10 patients due to C4/5 compression, in 6 patients due to C5/6 compression, and in 1 patient due to C6/7 compression. The modified Japanese Orthopedic Association scale (mJOA) was 12.71 ± 1.55 in the CSM group, with 4.87 ± 0.72 for sensory nerve function and 5.05 ± 1.35 for motor nerve function. For the control group, none of the volunteers had neurological dysfunction. T2 high signal was found at the most stenotic segment in 13 patients of the CSM group. Considering all the cervical segments, the aspect ratio (AUC = 0.823, $P = 0.001$, Sensitivity = 68.42%, Specificity = 82.47%) was more capable of determining the responsible segment than transverse ratio (AUC = 0.661, $P = 0.027$, Sensitivity = 68.42%, Specificity = 67.01%). AD, MD, and RD were significantly higher while FA was significantly lower in the responsible segment than in the irresponsible segment ($P < 0.05$). The AUC of DTI-Dorsal column parameters (AD, MD, RD, FA) was larger than the corresponding parameters of the DTI (Whole spinal cord). AD of DTI-Dorsal Column possessed the greatest efficacy (AUC = 0.823, sensitivity = 84.21%, specificity = 77.32%) to determine the responsible segment, larger than AD of DTI-Whole spinal cord (AUC = 0.822, $P = 0.001$, Sensitivity = 89.47%, Specificity = 77.32%), aspect ratio (AUC = 0.823, $P = 0.001$, Sensitivity = 68.42%, Specificity = 82.47%) and transverse ratio (AUC = 0.661, $P = 0.027$, Sensitivity = 68.42%, Specificity = 67.01%). Subgroup analysis revealed that the diagnostic efficacy of DTI and MRI parameters was influenced by cervical spine segment.

Conclusions When considering all cervical segments, AD from the DTI-Dorsal Column exhibited the most significant potential in identifying responsible segments. This potential was found to be superior to that of DTI-Whole spinal cord, aspect

Yanming Fang and Sisi Li contributed equally to the study.

Extended author information available on the last page of the article

ratio, the most stenotic segment, T2 high signals, transverse ratio, motor nerve dysfunction, and sensory nerve dysfunction. The diagnostic effectiveness of both DTI and MRI parameters was notably influenced by the specific cervical spine segment.

Keywords Diffusion tensor imaging (DTI) · Somatosensory evoked potential (SSEP) · Cervical spondylotic myelopathy (CSM) · Spinal cord electrophysiological examination · Receiver operating characteristic

Introduction

The presence of structural compression of the spinal cord and resultant neurological impairment often characterizes cervical spondylotic myelopathy (CSM) [1]. Age-related degeneration of the spine serves as the primary instigator of CSM, while spinal cord trauma and arthritis may also contribute to its development. Notably, the rate of CSM-related hospitalizations was reported at 4.04 per 100,000 person-years. Males and older persons have a higher incidence rate of CSM [2]. Nevertheless, variations in clinical evaluations, particularly neurological examination results, pose challenges in effectively assessing CSM patients. There is often a certain discrepancy between the degree of spinal cord compression and the symptoms experienced by the patient. Neurological function discrepancies may occur despite similar levels of spinal cord compression. In certain cases, patients with seemingly mild spinal cord compression on MRI exhibit pronounced limb numbness or even experience a loss of strength. The identification of responsible segments for neurological dysfunction proves to be complex in cases involving multi-stage compression, hindering accurate determination of the precise cervical spine segments necessitating surgical intervention. Previous studies have suggested that invasive spinal cord electrophysiological assessments offer an objective means of quantitatively evaluating spinal cord function and even pinpointing specific spinal cord segments [3, 4]. However, non-invasive assessment methods capable of precisely identifying neurological function at distinct spinal cord segments are currently unavailable.

Diffusion tensor imaging (DTI) is an advanced MR imaging method that quantitatively evaluates water molecule diffusion in the microenvironment of biological tissues, providing indirect insights into neurological function. This technique relies on measuring the thermal Brownian motion of water molecules. DTI finds extensive application in estimating brain axonal organization and assessing spinal cord function [5–7]. Commonly used DTI metrics for quantitative assessment include axial diffusivity (AD), mean diffusivity (MD), radial diffusivity (RD), and fractional anisotropy (FA). AD and FA are particularly crucial indicators for evaluating spinal cord function. AD represents the diffusion coefficient along the long axis of the diffusion tensor, typically aligned with the axon, and its value generally increases in compressed segments [8]. FA characterizes the water's anisotropic movement ability, typically displaying lower values in the compressed segments than in the normal segments [9].

Previous research has highlighted the significance of DTI metrics in diagnosing CSM. For instance, several studies have demonstrated a strong correlation between DTI and the modified Japanese Orthopedic Association scale (mJOA) [10–13]. Suetomi et al. specifically examined the diagnostic performance of maximum or minimum diffusion metrics (AD or FA) in specific CSM segments [14]. These studies could qualitatively determine CSM, while they have had limited success in pinpointing the exact cervical compression segment responsible for sensory neurological dysfunction. Moreover, most previous studies have relied on the relatively subjective mJOA scale for evaluating spinal cord function. The neurological function determination efficacy of mJOA is inferior to that of invasive electrophysiological [15–18].

Consequently, there is a need to validate the diagnostic efficacy of DTI metrics against electrophysiological neurological function examination. Validating the diagnostic efficacy of DTI metrics by assessing neurological function using electrophysiological neurological examinations is necessary. Therefore, our study aimed to validate the effectiveness of DTI metrics (AD, MD, RD, and FA) in diagnosing the specific segment responsible for somatic neurological dysfunction in CSM, employing electrophysiology as a tool to validate neurological function.

Material and methods

Basic information

Patients were enrolled based on the following criteria. Inclusion criteria included: (1) Patients with comprehensive examination data, including physical examination, imaging findings, and mJOA scale; (2) Patients who underwent intraoperative electrophysiological examination during posterior cervical spine surgery. Exclusion criteria included: (1) Patients under 18 years old; (2) Patients with a history of prior spinal surgery; (3) Patients with a history of tumors or tuberculosis; (4) Patients with a history of multiple traumas; (5) Patients with claustrophobia.

Following these criteria, 19 patients with CSM were included, along with 10 healthy individuals serving as controls with no symptoms or compressions observed on MRI examination between July 2020 and July 2021. The control group comprised 5 males and 5 females, while the CSM group included 10 males and 9 females (Table 1). The individuals in the control group were confirmed to be healthy through physical examination and MRI. In contrast, the CSM patients exhibited clinical neurological deficits and cervical spinal cord compression, as indicated by MRI findings.

The average age of all subjects was 56.14 ± 12.41 years, with an average BMI of 25.99 ± 3.87 kg/ m^2. The control group had an average age of 43.50 ± 7.21 years, while the CSM group had an average age of 62.79 ± 8.85 years. The BMI for the control group was 24.31 ± 2.91 kg/ m^2, compared to 26.79 ± 4.08 kg/ m^2 for the CSM patients. There were no statistically significant differences in gender distribution and BMI [(24.31 ± 2.91) kg/m^2 vs (26.79 ± 4.08) kg/m^2, ($P = 0.115$)] between the two groups. For blinded methodology, we blinded the healthy population and data measures. As the surgery was an invasive procedure and there was a clear difference between the control group and the patient group, the patients, the chief physician of the physical examination, and the operator were not blinded. This study was approved by the local Ethics Committee. Written informed consent was obtained from all subjects involved.

Clinical examination

Clinical routine physical examinations, including sensory nerve assessments, muscle strength evaluations, tendon reflex evaluations, and pathological reflex examinations, were conducted as evaluation references in both the control and CSM groups. These examinations were performed by a chief physician [X.H.] and a senior attending physician [JC.W.], both of whom specialize in the field of cervical disease. The mJOA scoring system was employed to quantify neurological function (**Appendix** Table 1).

Table 1 Demographic data of included cases

	Control	Patients	Statistics	*P*
Number	10	19		
Gender			Fisher's exact	1.000
Male	5	10		
Female	5	9		
Age (years)	43.50 ± 7.21	62.79 ± 8.85	t = − 5.92	< 0.001
BMI (kg/m^2)	24.31 ± 2.91	26.79 ± 4.08	t = − 1.63	0.115

BMI: Body Mass Index

Anatomical MRI and DTI data acquisition

Cervical spine anatomical MRI and DTI examination were conducted. For both the control group and CSM group, MRI scans were performed using a Philips 3.0 T Ingenia MRI scanner (Philips, Best, The Netherlands) equipped with a 16-channel head/neck coil. T1-weighted and T2-weighted axial and sagittal images were acquired with the following parameters. T1-weighted images were obtained with a repetition time of 400 ms, and an echo time (TE) of 6.85 ms. The field-of-view (FOV) is 250 × 250 mm^2, with an image resolution of 0.7 × 0.8 mm^2 and a slice thickness of 3-mm. Sagittal T2-weighted images were obtained with TE/TR = 100/3,000 ms, maintaining the same FOV and resolution as sagittal T1-weighted images. For axial T2-weighted images, the in-plane resolution is 0.9 × 0.9 mm^2 with a slice thickness of 4 mm, FOV = 190 × 190 mm^2, TE/TR = 70/5286 ms. The hyperintense signal on T2W MRI was assessed and identified by a radiologist and a chief physician [X.H.] from the spine department. The aspect ratio (defined as the anteroposterior diameter / the transverse diameter of the corresponding segment's spinal cord) and transverse ratio (defined as the transverse diameter of the corresponding segment's spinal cord / the transverse diameter of the spinal cord at C2/3) were calculated as the average of the results independently measured by two residents. Both residents conducted three repeated measurements to minimize measurement error (Fig. 1).

The DTI datasets were acquired using zonally-magnified oblique multislice echo planar imaging (ZOOM EPI) with a restricted FOV on the axial view. A total of twenty-three slices were scanned, covering spatial areas from C2 to C7. The specific imaging parameters were as follows: FOV = 56 × 42 mm^2, in-plane resolution = 0.88 × 0.88 mm^3, slice thickness = 4 mm, number of signal averaging (NSA) = 1, b = 0/800 s/mm^2, 32 diffusion directions, and TR = 4 heartbeats with peripheral pulse unit (PPU) triggering (trigger delay = 300 ms). The total scan time was approximately 5 min depending on the heart rate (Figs 2, 3, 4 and 5)

Data were processed using the Spinal Cord Toolbox [19] following a specific procedure. Initially, the diffusion dataset was automatically segmented and motion-corrected. Next, it was registered to the PAM50 template [20]. Subsequently, the DTI metrics were computed and tract-specific DTI metrics were extracted with various predefined regions of interest (ROIs) based on the atlas in the toolbox. Four ROIs were selected, including the whole spinal cord, dorsal columns, white matter, and gray matter**.** For quality control, the ROI definition was subsequently evaluated visually by overlaying the co-registered atlas template on the mean DWI image. Finally, morphologic features from anatomical MRI (e.g., aspect ratio, transverse ratio) and DTI metrics (AD, MD, RD, and FA) were then analyzed using the receiver operating

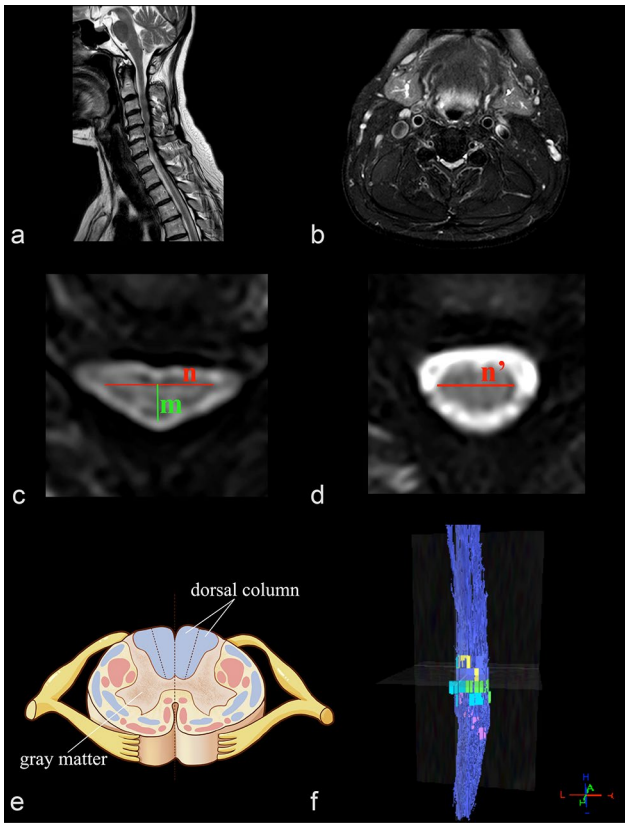

Fig. 1 Basic information and definitions of the parameters. **a** and **b** Conventional MRI of the cervical spine. **c** The aspect ratio was defined as the anteroposterior diameter (m) / the transverse diameter of the corresponding segment's spinal cord (n). **d** The transverse ratio was defined as the transverse diameter of the corresponding segment's spinal cord (n) / the transverse diameter of the spinal cord at C2/3 (n'). **e** The SCT spinal cord zoning diagram. **f** Demonstration of DTI spinal tractography

characteristic curve (ROC) to evaluate their diagnostic efficacy in determining the responsible segment of CSM.

Electrophysiological data acquisition and analysis

In the patients of the CSM group, intraoperative spinal cord electrophysiological examination was conducted for research purposes to assess spinal cord function during surgery. All CSM patients underwent spinous process splitting laminoplasty [21]. The operation procedures were as follows: A CSM patient was positioned in a prone posture under general anesthesia. A midline incision was made in the back of the neck to expose the spinous processes of segments C3–C7, while preserving the muscle insertion points of the C2 and C7 spinous processes. Subsequently, a single spinal cord deep electrode (PMT/2102-16-091, Chanhassen, MN, USA) was carefully positioned in the midline of the dural surface before decompression, allowing for the acquisition of electrophysiological signals in closer proximity to the spinal cord, thus enhancing result accuracy. The intraoperative monitoring system (Cascade 32 channels, North Kellogg St. Kennewick, WA, US) was used to collect the somatosensory evoked potentials (SSEP). Stimulation electrodes were placed on the median nerves of both wrists, using a stimulation intensity of 20 mA, a stimulation frequency of 4.13 Hz, 200 superimposition times, and a band-pass filter of 10–300 Hz. The electrode position was determined using C-arm radiographs. The responsible segment was determined as the spinal cord segment where the recorded potential exhibited the greatest decrease amplitude% or the largest prolonged latency% [22]. This electrophysiological examination served as an objective measure of neurological function.

Statistical analysis

The data were analyzed using Stata/MP 14.0 (College Station, TX, USA). One missing value in the control group's BMI was deleted. The Shapiro–Wilk normal distribution test was performed for the measurement data. Measurement data (age, BMI, mJOA scores) that conformed the normal distribution were expressed as mean ± standard deviation (SD). Independent samples *t*-tests were used for comparisons between the two groups. Data that did not meet the normal distribution were presented as the median and interquartile range (p25–p75) and were compared using the nonparametric Mann–Whitney U test between the two groups. Numerical data were expressed as percentages. Comparisons between the two groups were made using the Chi-square test or Fisher's exact test. Intraclass correlation coefficient (ICC) and Kappa were calculated for the assessment of intra/interobserver reliability. Additionally, the area under the curve (AUC), sensitivity, specificity, and Youden index% were computed to evaluate the diagnostic performance. All tests were two-sided, and *P* values less than 0.05 were considered significant.

Results

The responsible segment determined by electrophysiological examination.

According to the results of the electrophysiological examination, neurological dysfunction was found in 2 patients due to C3/4 compression, in 10 patients due to C4/5 compression, in 6 patients due to C5/6 compression, and in 1 patient due to C6/7 compression (Table 2).

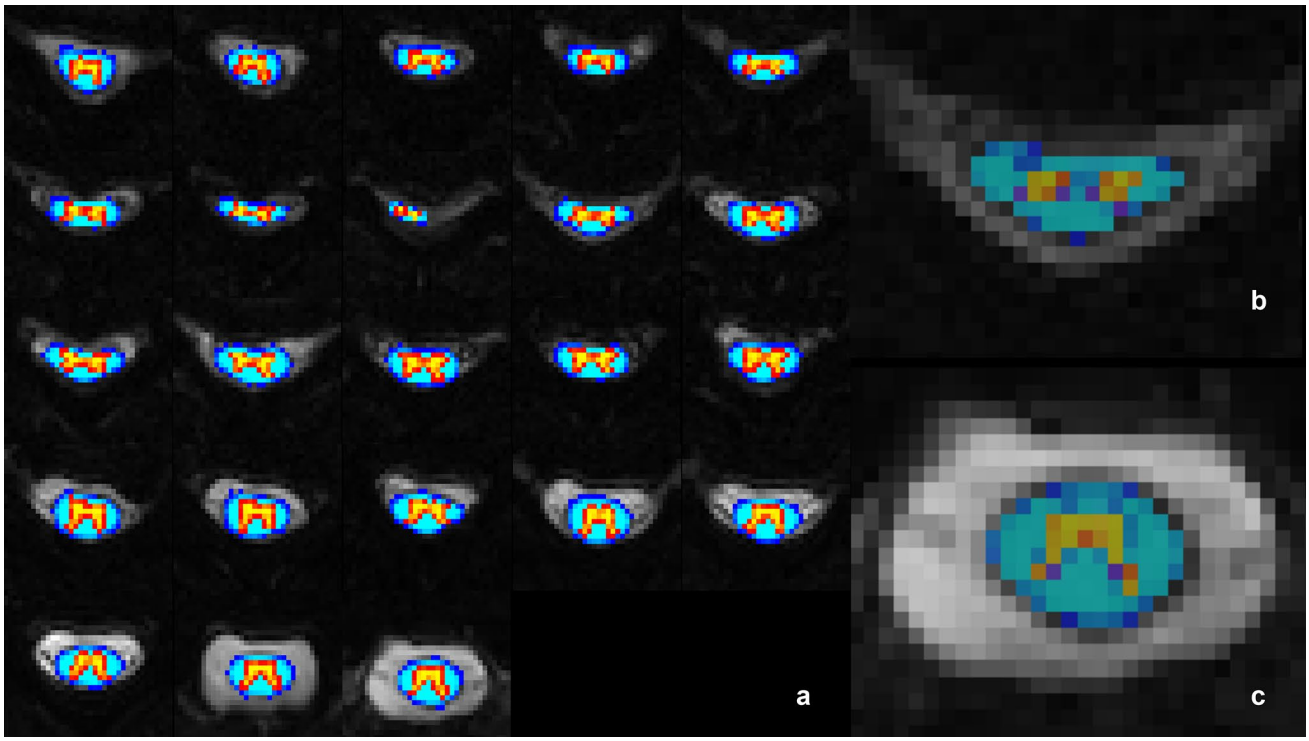

Fig. 2 **a** The automatic registration and segmentation results of the spinal cord for each slice from a particular patient. The co-registered white matter (depicted in blue) and gray matter (represented in yellow/red) were overlaid on the b0 image. The first slice was located at the C7 cervical vertebra, and the last slice was at C1. Note that the results were reliable for both the severely compressed slice **b** and the non-compressed slice **c**

The responsible segment determined by physical examination.

According to the results of the physical examination, sensory nerve dysfunction was found in 13 patients due to C3/4 compression, in 3 patients due to C4/5 compression, and in 2 patients due to C5/6 compression. One patient did not exhibit any sensory nerve dysfunction. (Table 2). Motor nerve dysfunction was found in 6 patients due to C3/4 compression, in 6 patients due to C4/5 compression, and in 2 patients due to C5/6 compression. Five patients did not exhibit any motor nerve dysfunction. The overall mJOA score in the CSM group was 12.71 ± 1.55. Specifically, the mJOA score for sensory nerve function was 4.87 ± 0.72, and the mJOA score for motor nerve function was 5.05 ± 1.35. In contrast, none of the volunteers in the control group exhibited any neurological dysfunction. The overall mJOA score was 17 in the control group. The average mJOA score of sensory nerve function was 6 and the average mJOA score of motor nerve function was 8.

Diagnostic efficacy of MRI parameters for the the responsible segment

According to anatomical MRI examination, the most stenotic segment was C3/4 in 7 patients, C4/5 in 7 patients, C5/6 in 4 patients, and C6/7 in one patient. T2 high signal was found in 13 patients at the most stenotic segment (Table 2). None of the volunteers in the control group had compression. Upon a comprehensive evaluation of all cervical segments, the aspect ratio (AUC = 0.823, $P = 0.001$, Sensitivity = 68.42%, Specificity = 82.47%) proves more effective than the transverse ratio (AUC = 0.661, $P = 0.027$, Sensitivity = 68.42%, Specificity = 67.01%) in identifying the specific responsible segment (Table 3). Further subgroup analysis revealed that the diagnostic efficacy of MRI parameters was influenced by cervical spine segment. Since there were fewer C3/4 and C6/7 responsible segments in this study, the subgroup analysis focused on C4/5 and C5/6 segments, which had a higher probability of compression according to clinical work. As for C4/5, AUC was 0.837 for the aspect ratio ($P = 0.003$, Sensitivity = 90.00%, Specificity = 73.68%) and 0.7 for the transverse ratio ($P = 0.081$, Sensitivity = 60.00%, Specificity = 94.74%). As for C5/6, AUC was 0.674 for the aspect ratio ($P = 0.196$, Sensitivity = 50.00%, Specificity = 89.96%) and 0.565 for the transverse ratio ($P = 0.628$, Sensitivity = 66.67%, Specificity = 56.52%), respectively.

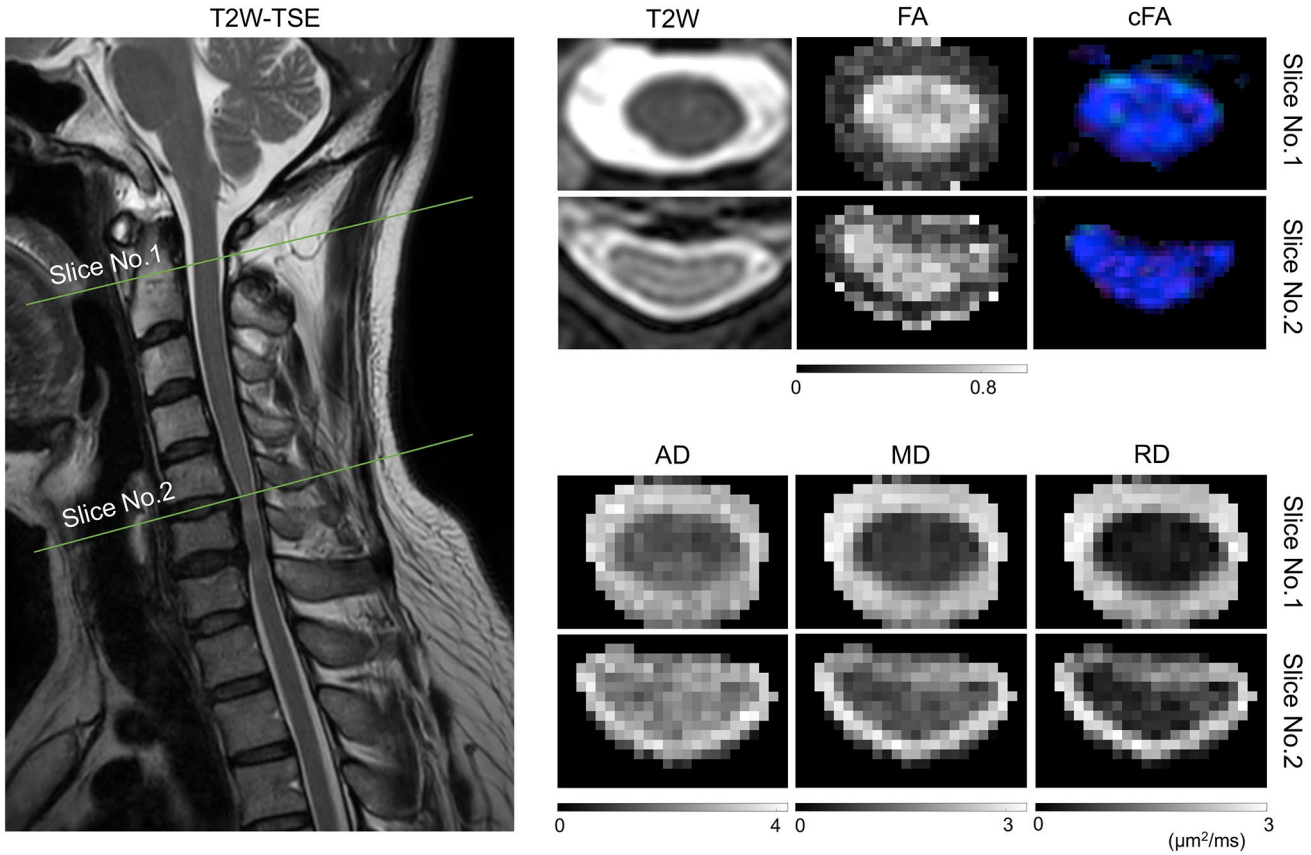

Fig. 3 The T2W anatomical MR image along with calculated DTI metrics and color encoded FA maps (cFA) for a non-compressed slice (Slice No. 1) and a compressed slice (Slice No. 2)

Diagnostic efficacy of the DTI metrics for the responsible segment

Among all DTI (Whole spinal cord) parameters, when taking all cervical segments into consider, AD (AUC = 0.822, $P = 0.001$, Sensitivity = 89.47%, Specificity = 77.32%) performed the best diagnostic efficacy, better than MD (AUC = 0.806, $P = 0.001$, Sensitivity = 78.95%, Specificity = 76.29%), RD (AUC = 0.783, $P = 0.001$, Sensitivity = 89.47%, Specificity = 60.82%) and FA (AUC = 0.750, $P = 0.001$, Sensitivity = 84.21%, Specificity = 54.64%) (Table 4). In subgroup analysis, for C4/5 subgroup, the AUC of the DTI metrics across the whole spinal cord were 0.732 for AD ($P = 0.044$), 0.768 for MD ($P = 0.019$), 0.742 for RD ($P = 0.035$), 0.726 for FA ($P = 0.049$), respectively. Similarly, for C5/6 subgroup, the AUC of the AD, MD, RD, and FA across the whole spinal cord was 0.949 ($P = 0.001$), 0.884 ($P = 0.004$), 0.848 ($P = 0.010$), 0.884 ($P = 0.004$), respectively.

Among all DTI (Dorsal column) parameters, when taking all cervical segments into consider, AD (AUC = 0.823, $P = 0.001$, Sensitivity = 84.21%, Specificity = 77.32%) performed the best diagnostic efficacy, better than MD (AUC = 0.816, $P = 0.001$, Sensitivity = 89.47%, Specificity = 71.13%), RD (AUC = 0.791, $P = 0.001$, Sensitivity = 89.47%, Specificity = 58.76%) and FA (AUC = 0.772, $P = 0.001$, Sensitivity = 73.68%, Specificity = 69.07%) (Table 5). In subgroup analysis, for the C4/5 subgroup, the AUC of the DTI measures in the dorsal column region are 0.732 for AD ($P = 0.044$), 0.763 for MD ($P = 0.022$), 0.747 for RD ($P = 0.031$), 0.737 for FA ($P = 0.039$), respectively. Similarly, for the C5/6 subgroup, the AUC of the DTI metrics for the dorsal column was 0.949 for AD ($P = 0.001$), 0.928 for MD ($P = 0.002$), 0.920 for RD ($P = 0.002$), 0.913 for FA ($P = 0.002$), respectively.

5. Summary of the effectiveness of non-invasive examinations (physical examination, anatomical MRI, DTI) in identifying the responsible cervical spine segment.

The segments identified as responsible through electrophysiological examination showed agreement with sensory nerve examination in 5 (26.32%) patients and with motor nerve examination in 7 (36.84%) patients.

Additionally, 11 (57.89%) patients with neurological dysfunction, based on the most stenotic segment on MRI, were consistent with the segments identified through electrophysiological examination. Similarly, ten (52.63%) segments

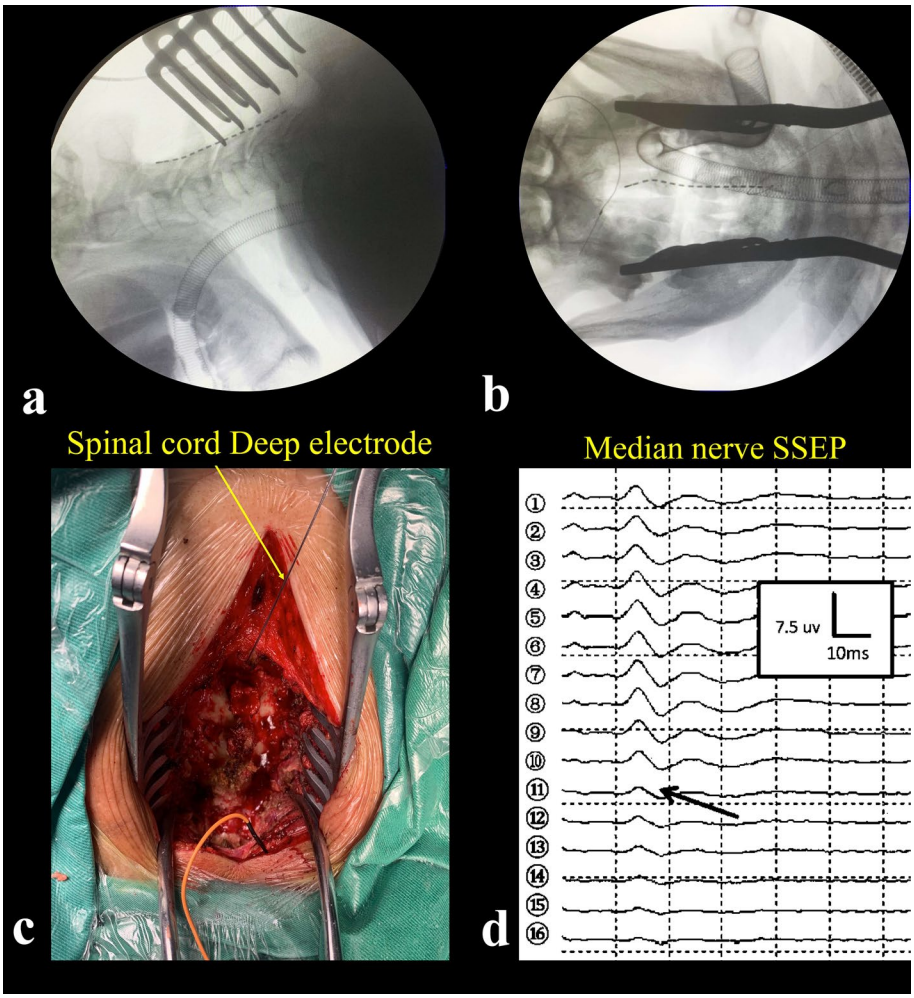

Fig. 4 Procedures of spinal cord electrophysiological examination. **a** and **b** showed radiographs after placing the deep spinal cord electrode on dura. **c** Placement of the spinal cord deep electrode. **d** Electrophysiological data of the patient. The greatest decrease of SSEP amplitude% could be seen at the 11th electrode points. The corresponding spinal cord segment was considered as the segment with the most serious impact on spinal cord function

exhibiting high signal on MRI were in concordance with the segments determined responsible by electrophysiology.

Comparing the responsible and irresponsible segments, it was found that AD, MD, and RD were significantly higher, whereas FA was significantly lower in the responsible segments compared to the irresponsible segments ($P < 0.05$). Overall, the AUC of DTI (Dorsal Column) parameters (AD, MD, RD, FA) was higher than the corresponding parameters of DTI (Whole spinal cord). Notably, axial diffusivity of DTI (Dorsal Column) exhibited the largest AUC (0.823), along with superior sensitivity (84.21%) and specificity (77.32%) among the parameters considered (Table 6). These results suggest that DTI (Dorsal Column) shows promising potential for determining responsible segments in non-invasive examinations.

Discussion

In the context of CSM with multiple segments of compression, the use of invasive intraoperative neurophysiological examination has proven valuable as a reliable and objective measure of spinal cord function. This method is essential as physical neurological examinations often struggle to precisely identify the specific responsible segment of compression that leads to neurological dysfunction. A study highlighted that SSEP revealed relatively fewer spinal segment functional abnormalities compared to the findings from traditional MRI, which primarily provided information on the anatomical structure of the spinal cord [23]. This suggested that not all compressed segments

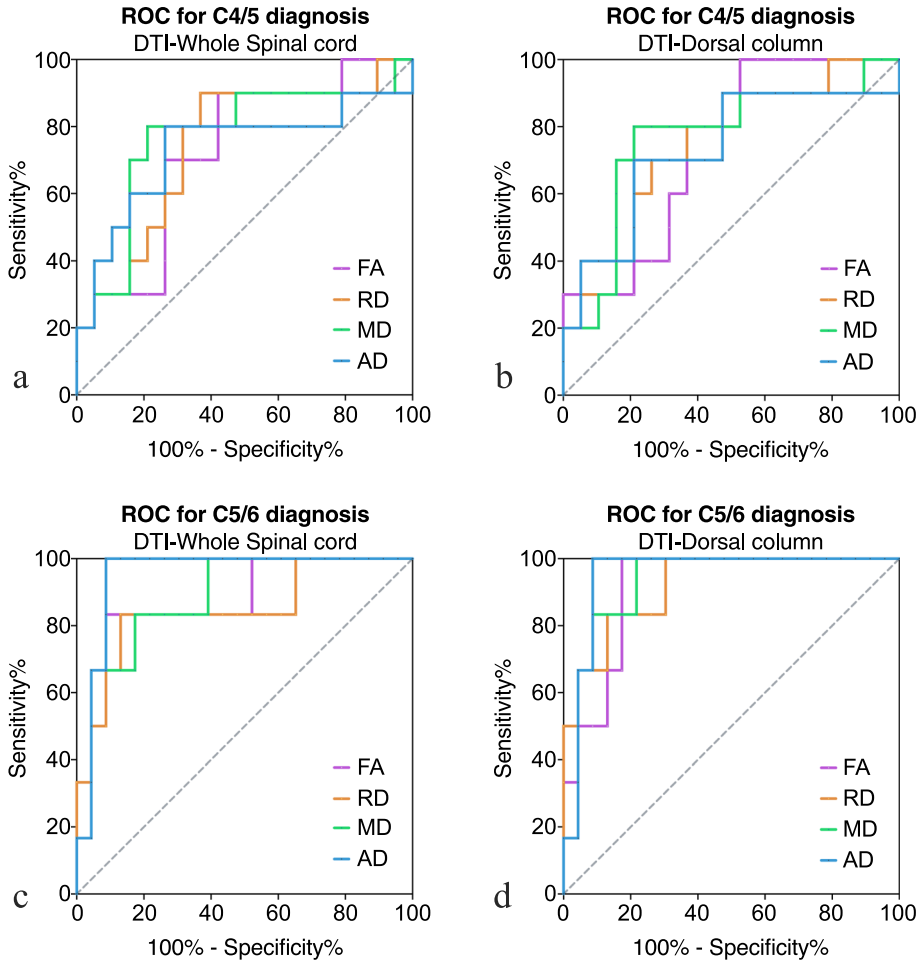

Fig. 5 ROC curves for the diagnosis of the responsible segment for CSM. **a** DTI metrics of whole spinal cord for C4/5. **b** DTI metrics of dorsal column for C4/5. **c** DTI metrics of whole spinal cord for C5/6. **d** DTI metrics of dorsal column for C5/6. ROC: receiver operating characteristic

contribute to the observed neurological dysfunction. In scenarios where multiple segments are compressed, it is possible that only one segment primarily contributes to the spinal cord dysfunction. Hence, identifying the precise responsible spinal cord segment affecting nerve function becomes crucial for making well-informed and appropriate surgical decisions.

Several studies have focused on assessing the diagnostic performance of DTI met for CSM by reporting sensitivity and specificity. The most extensively studied FA and AD were discussed here [14, 24]. Wang's study reported a sensitivity of 30.77% and specificity of 91.89% for the FA to identify myelopathic segments in CSM [25]. Our results were much better in some ways (DTI-dorsal column, sensitivity = 73.68%, specificity = 69.07%, Youden index = 42.75%). Furthermore, it has been reported that FA exhibits the largest AUC of 0.750 [24], which was lower than our results (AUC: AD = 0.823, FA = 0.772). Few studies computed the AUC to assess the efficacy of DTI in diagnosing CSM. To some extent, CSM can be considered as a chronic neurological injury [26]. To provide further context, we also considered DTI findings from cases of cervical spine injuries for comparison. Previous studies have indicated that in cases of spinal cord injury, FA (AUC = 0.770) at the lesion epicenter could effectively discriminate injury severity [27]. Moreover, when combining FA, AD, and RD, the AUC was reported to be 0.92 for diagnosing cervical spine injury [28]. Notably, the results of series or parallel diagnostic examinations using FA and AD were less effective compared to those using FA or AD alone. However, it is important to acknowledge the differences that exist between acute spinal cord injury and CSM.

In addition, our study involved the utilization of the Spinal Cord Toolbox (SCT) to partition the nerve conduction tracts of the spinal cord and measure the corresponding DTI metrics. Interestingly, we discovered that, in comparison between the whole spinal cord and the dorsal column tract (includes the fasciculus cuneatus and fasciculus gracilis), the dorsal tract exhibited superior diagnostic performance to the whole spinal cord. This finding is in line with the results of a study conducted by Jan Valošek et al.[18]. Different results between spinal cord tracts may be related to the pathogenesis of the disease, as in clinical practice, the sensory function is usually the initial problem. This might

Table 2 Responsible segment for the neurological dysfunction determined by different methods of CSM group

No. of Patients	Gender	Median- SSEP	Sensory nerve examination	Motor nerve examination	MRI—The Most Stenotic Segment	MRI- Stenotic Segments	T2 High signal on MRI	m-JOA Score (sensor)	m-JOA Score (motor)	m-JOA Score (pre-operation)
1	F	C5/6	C5/6	ND	C5/6	C3/4-C5/6	C4/5, C5/6	4	3.5	10.5
2	M	C5/6	C3/4	C3/4	C4/5	C3/4-C4/5	C4/5	5	4.5	12.5
3	F	C4/5	C3/4	C3/4	C4/5	C2/3-C5/6	C4/5	4	5	12
4	M	C4/5	C3/4	C4/5	C3/4	C3/4-C5/6	C3/4, C4/5, C5/6	5	6.5	14.5
5	F	C4/5	C3/4	ND	C5/6	C4/5-C5/6	–	5.5	4.5	13
6	M	C4/5	C3/4	ND	C3/4	C2/3-C6/7	–	5	6.5	12.5
7	F	C6/7	C3/4	C4/5	C6/7	C2/3-C6/7	C6/7	5	3.5	11.5
8	M	C3/4	C3/4	ND	C3	C2/3-C4/5	C3/4	5.5	5.5	12
9	M	C4/5	ND	C3/4	C4/5	C4/5-C6/7	–	6	7	16
10	F	C4/5	C3/4	C4/5	C4/5	C3/4-C6/7	–	4.5	5.5	13
11	M	C3/4	C3/4	C3/4	C3/4	C3/4-C5/6	C3/4	5	2	10
12	M	C5/6	C3/4	C3/4	C4/5	C3/4-C5/6	C3/4	4.5	5.5	13
13	F	C5/6	C4/5	C4/5	C3/4	C3/4-C4/5	C3/4	5.5	5.5	14
14	M	C5/6	C5/6	C5/6	C5/6	C5/6	C5/6	4	3.5	10.5
15	F	C4/5	C4/5	C4/5	C4/5	C3/4-C5/6	C4/5, C5/6	3	6	12
16	M	C4/5	C3/4	C3/4	C3/4	C3/4-C5/6	C3/4	5.5	4	12.5
17	F	C4/5	C3/4	ND	C4/5	C4/5-C6/7	C4/5	5	7	15
18	M	C4/5	C4/5	C4/5	C3/4	C3/4-C6/7	C3/4, C4/5	5.5	4.5	13
19	F	C5/6	C3/4	C5/6	C5/6	C4/5-C6/7	–	5	6	14

SSEP: somatosensory evoked potential, ND: not determined; –: None high signal

Table 3 Diagnosis efficacy of anatomical MRI parameters in determining responsible segment

		Non-responsible segment	Responsible segment	AUC	*P*	Sensitivity%	Specificity%	Youden index%	Cut-off Value
C overall	Aspect ratio	0.366 (0.299–0.421)	0.245 (0.204–0.329)	0.823	0.001	68.42	82.47	50.89	0.287
	Transverse ratio	1.074 (0.966–1.122)	1.121 (1.029–1.239)	0.661	0.027	68.42	67.01	35.43	1.106
C3/4	Aspect ratio	0.368 (0.256–0.429)	0.171 (0.135–0.207)	0.963	0.031	100	92.59	92.59	0.215
	Transverse ratio	1.082 (1.058–1.118)	0.969 (0.890–1.048)	0.870	0.085	100	63.30	63.30	81.48
C4/5	Aspect ratio	0.367 (0.296–0.425)	0.238 (0.204–0.286)	0.837	0.003	90.00	73.68	63.68	0.308
	Transverse ratio	1.164 (1.093–1.203)	1.228 (1.121–1.263)	0.700	0.081	60.00	94.74	54.74	1.215
C5/6	Aspect ratio	0.345 (0.294–0.397)	0.304 (0.211–0.359)	0.674	0.196	50.00	89.96	39.96	0.268
	Transverse ratio	1.074 (1.006–1.183)	1.111 (1.029–1.146)	0.565	0.628	66.67	56.52	23.19	1.097
C6/7	Aspect ratio	0.369 (0.349–0.429)	0.333 (0.333–0.333)	0.821	0.282	100	82.14	82.14	0.338
	Transverse ratio	0.895 (0.790–0.982)	0.857 (0.857–0.857)	0.607	0.720	100	60.71	60.71	0.858

AUC: Area under the curve. *P*: *P*-value of the AUC. Youden index: Sensitivity + Specificity – 1

also be related to the use of SSEP which was generated from the dorsal sensory functional area as an evaluation function index in our electrophysiological studies. In our study, when considering all cervical segments, AD from the DTI-Dorsal Column exhibited the most significant potential in identifying responsible segments, superior to parameters of DTI-Whole spinal cord, aspect ratio, the most stenotic segment, T2 high signals, transverse ratio, motor nerve dysfunction, and sensory nerve dysfunction. These results suggested that AD from DTI (Dorsal Column) showed promising potential for determining responsible segments in non-invasive examinations (Table 6).

The discrepancies observed between our study and other existing research may be attributed to the use of different standards for assessing spinal cord function. While previous DTI studies primarily relied on the mJOA score as the standard for evaluating spinal cord function [24]. Our study employed intraoperative neurophysiological monitoring as an invasive examination method to detect neurological function, rather than relying solely on the mJOA score [14]. Notably, the direct attachment of the probe to the surface of the spinal cord during our intraoperative neurophysiological monitoring resulted in reduced signal interference. This approach enhanced the objectivity of neurological function evaluation compared to the use of the mJOA score alone. During cervical spine surgery, we recorded SSEP generated from the dorsal sensory functional area of the spinal cord at the corresponding cervical spine segment. The electrodes we used were positioned closer to the source of the generated neurological signals compared to electrodes placed on the scalp, thereby reducing noise signals from specific structures along the pathway [29, 30]. Consequently, changes in the amplitude or latency of the potential may be more sensitive in reflecting the degree of neuronal damage in the spinal cord caused by mechanical compression [31]. These methodological differences may have contributed to the variations observed between our study and previous research.

Additionally, our study highlighted that the diagnostic efficacy of both DTI and MRI parameters was significantly influenced by the specific segment of the cervical spine. Notably, our clinical observations consistently indicated that patients with disc herniation at the C4/5 or C5/6 level were more prevalent. Interestingly, based on our findings, the diagnostic efficacy of MRI and DTI in assessing neurological deficits at the higher segment (C4/5) were similar. Conversely, when diagnosing neurological dysfunction resulting from the lower segment (C5/6), DTI exhibited a generally superior diagnostic effect compared to anatomical MRI. Several factors potentially accounted for this discrepancy. Firstly, it is commonly observed that CSM patients often suffer from compression in multiple segments. The impact of the upper segment's compression might have an additive effect on the DTI metrics of the lower segment, leading to more statistically significant results in the lower segment. Secondly, the degree of compression at the C4/5 level was notably higher than

Table 4 Diagnosis efficacy of DTI (Whole spinal cord) parameters in determining responsible segment

		Non-responsible segment	Responsible segment	AUC	*P*	Sensitivity%	Specificity%	Youden index%	Cut-off Value
C Overall	AD [mm^2/s]	1.761 (1.705–1.858) $*10^{-3}$	2.046 (1.948–2.123) $*10^{-3}$	0.822	0.001	89.47	77.32	66.79	1.875 $*10^{-3}$
	MD [mm^2/s]	0.958 (0.895–1.050) $*10^{-3}$	1.168 (1.056–1.299) $*10^{-3}$	0.806	0.001	78.95	76.29	55.24	1.053 $*10^{-3}$
	RD [mm^2/s]	0.546 (0.475–0.658) $*10^{-3}$	0.718 (0.610–0.961) $*10^{-3}$	0.783	0.001	89.47	60.82	50.29	0.582 $*10^{-3}$
	FA	0.663 (0.602–0.705)	0.580 (0.471–0.648)	0.750	0.001	84.21	54.64	38.85	0.655
C3/4	AD [mm^2/s]	1.832 (1.747–1.941) $*10^{-3}$	1.976 (1.906–2.046) $*10^{-3}$	0.741	0.263	100	62.96	62.96	1.888 $*10^{-3}$
	MD[mm^2/s]	0.952 (0.895–1.046) $*10^{-3}$	1.069 (1.000–1.137) $*10^{-3}$	0.722	0.302	100	62.96	62.96	1.000$*10^{-3}$
	RD [mm^2/s]	0.511 (0.460–0.604) $*10^{-3}$	0.671 (0.589–0.752) $*10^{-3}$	0.796	0.169	100	74.07	74.07	0.581 $*10^{-3}$
	FA	0.703 (0.644–0.715)	0.581 (0.566–0.596)	0.944	0.039	100	92.59	92.59	0.599
C4/5	AD [mm^2/s]	1.783 (1.718–2.002) $*10^{-3}$	2.082 (1.976–2.155) $*10^{-3}$	0.732	0.044	80.00	73.68	53.68	1.950 $*10^{-3}$
	MD [mm^2/s]	0.934 (0.872–1.089) $*10^{-3}$	1.150 (1.093–1.299) $*10^{-3}$	0.768	0.019	80.00	78.95	58.95	1.091 $*10^{-3}$
	RD [mm^2/s]	0.500 (0.426–0.660) $*10^{-3}$	0.670 (0.610–0.961) $*10^{-3}$	0.742	0.035	90.00	63.16	53.16	0.565 $*10^{-3}$
	FA	0.693 (0.615–0.727)	0.642 (0.519–0.674)	0.726	0.049	90.00	57.89	47.89	0.680
C5/6	AD [mm^2/s]	1.732 (1.675–1.821) $*10^{-3}$	2.030 (1.948–2.069) $*10^{-3}$	0.949	0.001	100.00	91.30	91.30	1.869 $*10^{-3}$
	MD [mm^2/s]	0.988 (0.884–1.032) $*10^{-3}$	1.181 (1.056–1.253) $*10^{-3}$	0.884	0.004	83.33	82.61	65.94	1.047 $*10^{-3}$
	RD [mm^2/s]	0.575 (0.489–0.644) $*10^{-3}$	0.802 (0.676–0.848) $*10^{-3}$	0.848	0.010	83.33	86.96	70.29	0.674 $*10^{-3}$
	FA	0.653 (0.598–0.669)	0.548 (0.469–0.580)	0.884	0.004	83.33	91.30	74.63	0.581
C6/7	AD [mm^2/s]	1.747 (1.677–1.812) $*10^{-3}$	2.024 (2.024–2.024) $*10^{-3}$	0.929	0.152	100	92.86	92.86	1.973 $*10^{-3}$
	MD [mm^2/s]	0.951 (0.908–1.061) $*10^{-3}$	1.381 (1.381–1.381) $*10^{-3}$	0.964	0.120	100	96.43	96.43	1.359 $*10^{-3}$
	RD [mm^2/s]	0.573 (0.523–0.705) $*10^{-3}$	1.060 (1.060–1.060) $*10^{-3}$	1.000	0.094	100	100	100	1.007 $*10^{-3}$
	FA	0.616 (0.561–0.672)	0.386 (0.386–0.386)	1.000	0.094	100	100	100	0.449

AD: Axial Diffusivity. MD: Mean Diffusivity. RD: Radial Diffusivity. FA: Fractional Anisotropy. AUC: Area under the curve. *P*: *P*-value of the AUC. Youden index: Sensitivity + Specificity − 1

that at the C5/6 level in our study (aspect ratio: 0.238 (0.204–0.286) versus 0.304 (0.211–0.359); transverse ratio: 1.228 (1.121–1.263) versus 1.111 (1.029–1.146)). This discrepancy might indicate that DTI metrics possess a higher diagnostic utility in confirming responsible segments compared to anatomical MRI parameters, particularly in patients with milder compression. This finding could assist surgeons in choosing appropriate surgical segments and minimizing surgical injury. In cases of more severe compression, the responsible segment might be multiple, necessitating more extensive multi-segment surgery.

There are several limitations in this study. Firstly, a notable statistical difference in age ($t = -5.92$, $P < 0.001$) was observed between the two groups. While some studies have reported that DTI values are not significantly influenced by age in subjects older than 40 years ($P < 0.05$) [32–34], it is still imperative to consider an age-matched cohort for more conclusive findings in future studies. Secondly, to further explore the diagnostic efficacy under various degrees of compression, it is crucial to grade the severity of compression. Lastly, it should be noted that the members of the healthy control group were confirmed to be in good health and without cervical disorders only based on physical

Table 5 Diagnosis efficacy of DTI (Dorsal column) parameters in determining responsible segment

		Non-responsible segment	Responsible segment	AUC	*P*	Sensitivity%	Specificity%	Youden index%	Cut-off Value
C Overall	AD [mm^2/s]	1.876 (1.780–2.004) $*10^{-3}$	2.143 (2.040–2.301) $*10^{-3}$	0.823	0.001	84.21	77.32	61.53	2.037 * 10^{-3}
	MD [mm^2/s]	0.977 (0.892–1.052) $*10^{-3}$	1.197 (1.062–1.327) $*10^{-3}$	0.816	0.001	89.47	71.13	60.60	1.037 $*10^{-3}$
	RD [mm^2/s]	0.496 (0.415–0.629) $*10^{-3}$	0.729 (0.588–0.893) $*10^{-3}$	0.791	0.001	89.47	58.76	48.23	0.537 $*10^{-3}$
	FA	0.716 (0.656–0.763)	0.614 (0.515–0.689)	0.772	0.001	73.68	69.07	42.75	0.672
C3/4	AD [mm^2/s]	1.966 (1.797–2.100) $*10^{-3}$	2.110 (2.110–2.110) $*10^{-3}$	0.815	0.143	100	81.48	81.48	2.108 $*10^{-3}$
	MD [mm^2/s]	0.968 (0.891–1.053) $*10^{-3}$	1.124 (1.039–1.209) $*10^{-3}$	0.796	0.169	100	70.37	70.37	1.033 $*10^{-3}$
	RD [mm^2/s]	0.478 (0.359–0.606) $*10^{-3}$	0.648 (0.538–0.759) $*10^{-3}$	0.796	0.169	100	62.96	62.96	0.529 $*10^{-3}$
	FA	0.738 (0.701–0.803)	0.645 (0.601–0.689)	0.889	0.071	100	81.48	81.48	0.694
C4/5	AD [mm^2/s]	1.895 (1.836–2.036) $*10^{-3}$	2.092 (1.932–2.301) $*10^{-3}$	0.732	0.044	70.00	78.95	48.95	2.037 $*10^{-3}$
	MD [mm^2/s]	0.993 (0.894–1.044) $*10^{-3}$	1.156 (1.047–1.275) $*10^{-3}$	0.763	0.022	80.00	78.95	58.95	1.045 $*10^{-3}$
	RD [mm^2/s]	0.480 (0.412–0.604) $*10^{-3}$	0.627 (0.544–0.893) $*10^{-3}$	0.747	0.031	70.00	73.68	43.68	0.579 $*10^{-3}$
	FA	0.737 (0.634–0.765)	0.669 (0.516–0.717)	0.737	0.039	100.00	47.37	47.37	0.742
C5/6	AD [mm^2/s]	1.817 (1.756–1.951) $*10^{-3}$	2.201 (2.060–2.252) $*10^{-3}$	0.949	0.001	100.00	91.30	91.30	2.039 $*10^{-3}$
	MD [mm^2/s]	0.942 (0.887–1.035) $*10^{-3}$	1.238(1.131–1.327) $*10^{-3}$	0.928	0.002	100.00	78.26	78.26	1.048 $*10^{-3}$
	RD [mm^2/s]	0.489 (0.415–0.617) $*10^{-3}$	0.806 (0.651–0.866) $*10^{-3}$	0.920	0.002	83.33	86.96	70.29	0.647 $*10^{-3}$
	FA	0.715(0.674–0.736)	0.588 (0.437–0.614)	0.913	0.002	100.00	82.61	82.61	0.657
C6/7	AD [mm^2/s]	0.183 (0.173–0.196) $*10^{-3}$	0.281 (0.281–0.281) $*10^{-3}$	1.000	0.094	100.00	100.00	100.00	2.693 $*10^{-3}$
	MD [mm^2/s]	0.992 (0.905–1.113) $*10^{-3}$	1.609 (1.609–1.609) $*10^{-3}$	1.000	0.094	100.00	100.00	100.00	1.541 $*10^{-3}$
	RD [mm^2/s]	0.557 (0.465–0.703) $*10^{-3}$	1.006 (1.006–1.006) $*10^{-3}$	1.000	0.094	100.00	100.00	100.00	0.966 $*10^{-3}$
	FA	0.668 (0.607–0.728)	0.515 (0.515–0.515)	1.000	0.094	100.00	100.00	100.00	0.529

AD: Axial Diffusivity. MD: Mean Diffusivity. RD: Radial Diffusivity. FA: Fractional Anisotropy. AUC: Area under the curve. *P*: *P*-value of the AUC. Youden index: Sensitivity + Specificity − 1

examination and MRI, electrophysiological testing was not conducted due to ethical considerations.

Conclusion

When considering all cervical segments, AD from the DTI-Dorsal Column exhibited the most significant potential in identifying responsible segments. This potential was found to be superior to that of DTI-Whole spinal cord, aspect ratio, the most stenotic segment, T2 high signals, transverse ratio, motor nerve dysfunction, and sensory nerve dysfunction. The diagnostic effectiveness of both DTI and MRI parameters was notably influenced by the specific cervical spine segment.

Table 6 Summary of Diagnostic efficacy MRI and DTI for the responsible segment

Examination methods		AUC	P	Sensitivity%	Specificity%	Youden index%
Physical examination	Sensory nerve dysfunction			26.32	86.60	12.92
	Motor nerve dysfunction			36.84	92.78	29.62
MRI	The most stenotic segment			57.89	91.75	49.64
	T2 high signals			52.63	90.72	43.35
	Aspect ratio	0.823	0.001	68.42	82.47	50.89
	Transverse ratio	0.661	0.027	68.42	67.01	35.43
DTI (Whole spinal cord)	AD	0.822	0.001	89.47	77.32	66.79
	MD	0.806	0.001	78.95	76.29	55.24
	RD	0.783	0.001	89.47	60.82	50.29
	FA	0.750	0.001	84.21	54.64	38.85
DTI (Dorsal column)	AD	0.823	0.001	84.21	77.32	61.53
	MD	0.816	0.001	89.47	71.13	60.60
	RD	0.791	0.001	89.47	58.76	48.23
	FA	0.772	0.001	73.68	69.07	42.75

AD: Axial Diffusivity. MD: Mean Diffusivity. RD: Radial Diffusivity. FA: Fractional Anisotropy. AUC: Area under the curve. *P*: *P*-value of the AUC. Youden index : Sensitivity + Specificity − 1

Appendix Table 1. Modified japanese orthopedic association score.

1. Motor function	
A. Upper extremity motor function	
0	Impossible to eat with chopsticks or spoons
1	Possible to eat with spoons but not with chopsticks
2	Possible to eat with chopsticks, but to a limited degree
3	Possible to eat with chopsticks, awkward
4	No disability
B. Shoulder and elbow motor function	
-2	Deltoid or biceps strength ≤ 2, contraction against gravity eliminated or even worse
-1	Deltoid or biceps strength = 3, contraction against gravity only
-0.5	Deltoid or biceps strength = 4, contraction against gravity and slight resistance
0	Deltoid or biceps strength = 5, contraction against gravity and full resistance
C. Lower extremity motor function	
0	Cannot walk
0.5	Can stand
1	Needs cane or aid on flat ground
1.5	Can walk without cane or aid but unsteadily
2	Needs cane or aid only on stairs
2.5	Needs cane or aid walk downstairs
3	Can walk without a cane or aid but slowly
4	No disability
2. Sensory function	
A. Upper extremity	
0	Apparent sensory loss
0.5	Between apparent and minimal sensory loss
1	Minimal sensory loss
1.5	Between normal and minimal sensory loss
2	Normal
B. Trunk (same as A)	
C. Lower extremity (same as A)	
3. Bladder function	
0	Complete retention
1	Severe disturbance
2	Mild disturbance
3	Normal

Appendix Table 2. Basic information and m-JOA scores of the control group

No. of volunteers	Gender	m-JOA score (sensor)	m-JOA score (motor)	m-JOA score (pre-operation)
1	M	6	8	17
2	M	6	8	17

No. of volunteers	Gender	m-JOA score (sensor)	m-JOA score (motor)	m-JOA score (pre-operation)
3	M	6	8	17
4	M	6	8	17
5	F	6	8	17
6	F	6	8	17
7	F	6	8	17
8	F	6	8	17
9	F	6	8	17
10	M	6	8	17

Appendix Table 3. Intra/interobserver reliability measures

Variables	Intra-observer reliability		Inter-observer reliability	
	Test statistic	95% CI	Test statistic	95% CI
mJOA scores	ICC = 1		N/A	N/A
Aspect ratio				
Rater1	ICC = 0.998	[0.970, 0.999]	ICC = 0.997	[0.850, 0.999]
Rater2	ICC = 0.992	[0.884, 0.997]		
Transverse ratio				
Rater1	ICC = 0.987	[0.851, 0.996]	ICC = 0.991	[0.647, 0.998]
Rater2	ICC = 0.988	[0.849, 0.996]		
The most stenotic segment	N/A	N/A	Kappa = 1	
T2 high signals	N/A	N/A	Kappa = 1	

ICC: Intraclass correlation coefficient (two-way random-effects model, absolute agreement). CI 95%: confidence interval of 95%.

Funding CAMS Innovation Fund for Medical Sciences, code: 2021-I2M-5-007. Capital's Funds for Health Improvement and Research, code: CFH2020-2-1121. Beijing Jishuitan Hospital Elite Young Scholar Programme, code: XKGG202103. National Natural Science Foundation of China, code: 11,871,459. Beijing Hospitals Authority Innovation Studio of Young Staff Funding Support, code: 202109.

Data availability The datasets used and/or analyzed during the current study are available from the corresponding author on reasonable request. The work has not been published previously, is approved by all authors and explicitly by the responsible authorities where the work was carried out. If accepted, it will not be published elsewhere in the same form, in English or in any other language, including electronically without the written consent of the copyright-holder ported in this paper.

Declarations

Conflict of interest The authors declare that they have no known competing financial interests or personal relationships that could have appeared to influence the work. The authors declare that there was No financial support for the study.

Ethics approval All procedures performed in studies involving human participants were in accordance with the ethical standards of the institutional committee and with the 1964 Helsinki Declaration and its later amendments or comparable ethical standards. The study was approved by the ethical Committee of the Beijing jisuhitan Hospital.

Informed consent Informed consent was obtained from all individual participants included in the study.

Consent to publish The participant has consented to the submission to the journal.

Consent for publication Images are entirely unidentifiable and there are no details on individuals reported within the manuscript.

References

1. Ferrara LA (2012) The biomechanics of cervical spondylosis. Adv orthop. https://doi.org/10.1155/2012/493605
2. Wu JC et al (2013) Epidemiology of cervical spondylotic myelopathy and its risk of causing spinal cord injury: a national cohort study. Neurosurg Focus 35(1):E10
3. Kerkovský M et al (2012) Magnetic resonance diffusion tensor imaging in patients with cervical spondylotic spinal cord compression: correlations between clinical and electrophysiological findings. Spine 37(1):48–56
4. Martin AR et al (2021) Imaging and electrophysiology for degenerative cervical myelopathy [AO Spine RECODE-DCM research priority number 9]. Glob Spine J 12(1):130S-146S
5. Mori S, Zhang J (2006) Principles of diffusion tensor imaging and its applications to basic neuroscience research. Neuron 51(5):527–539
6. Song T et al (2011) Diffusion tensor imaging in the cervical spinal cord. Eur Spine J 20(3):422–428
7. Sąsiadek MJ, Szewczyk P, Bladowska J (2012) Application of diffusion tensor imaging (DTI) in pathological changes of the spinal cord. Med Sci Monit 18(6):Ra73–Ra79
8. Facon D et al (2005) MR diffusion tensor imaging and fiber tracking in spinal cord compression. Am J Neuroradiol 26(6):1587–1594
9. Yoo W-K et al (2013) Correlation of magnetic resonance diffusion tensor imaging and clinical findings of cervical myelopathy. Spine J 13(8):867–876
10. Ellingson BM et al (2014) Diffusion tensor imaging predicts functional impairment in mild-to-moderate cervical spondylotic myelopathy. Spine J 14(11):2589–2597
11. Cloney MB, Smith ZA, Weber KA (2018) Quantitative magnetization transfer MRI measurements of the anterior spinal cord region are associated with clinical outcomes in cervical spondylotic myelopathy. Spine 43(10):675

12. Han X et al (2020) The evaluation and prediction of laminoplasty surgery outcome in patients with degenerative cervical myelopathy using diffusion tensor MRI. Am J Neuroradiol 41(9):1745–1753
13. Wen CY et al (2014) Is diffusion anisotropy a biomarker for disease severity and surgical prognosis of cervical spondylotic myelopathy? Radiology 270(1):197–204
14. Suetomi Y et al (2016) Application of diffusion tensor imaging for the diagnosis of segmental level of dysfunction in cervical spondylotic myelopathy. Spinal Cord 54(5):390–395
15. Wen C-Y et al (2014) Diffusion tensor imaging of somatosensory tract in cervical spondylotic myelopathy and its link with electrophysiological evaluation. Spine J 14(8):1493–1500
16. Fehlings, MG, et al. (2017) A clinical practice guideline for the management of degenerative cervical myelopathy: introduction, rationale, and scope. Sage Publications Sage CA: Los Angeles, CA. p. 21S-27S
17. Bednarik J et al (2008) Presymptomatic spondylotic cervical myelopathy: an updated predictive model. Eur Spine J 17(3):421–431
18. Valošek J et al (2021) Diffusion magnetic resonance imaging reveals tract-specific microstructural correlates of electrophysiological impairments in non-myelopathic and myelopathic spinal cord compression. Eur J Neurol 28(11):3784–3797
19. De Leener B et al (2017) SCT: spinal cord toolbox, an open-source software for processing spinal cord MRI data. Neuroimage 145:24–43
20. De Leener B et al (2018) PAM50: Unbiased multimodal template of the brainstem and spinal cord aligned with the ICBM152 space. Neuroimage 165:170–179
21. Tian W, WH, (2013) Cervical LAMINOPLASTY and SLAC surgery. Chin J Bone Joint Surg. (s1):1-10.
22. Park JH, Hyun SJ (2015) Intraoperative neurophysiological monitoring in spinal surgery. World J Clin Cases 3(9):765–773
23. Tanaka N et al (2005) Functional diagnosis using multimodal spinal cord evoked potentials in cervical myelopathy. J Orthop Sci 10(1):3–7
24. Shen C et al (2018) Value of conventional MRI and diffusion tensor imaging parameters in predicting surgical outcome in patients with degenerative cervical myelopathy. J Back Musculoskelet Rehabil 31(3):525–532
25. Wang SQ et al (2015) Prediction of myelopathic level in cervical spondylotic myelopathy using diffusion tensor imaging. J Magn Reson Imaging 41(6):1682–1688
26. Kanchiku T et al (2016) Correlation between spinal cord function assessed by intraoperative SCEPs and morphology of the compressed spinal cord on MRI. Clin spine surg 29(10):E496–E501
27. Poplawski MM et al (2019) Application of diffusion tensor imaging in forecasting neurological injury and recovery after human cervical spinal cord injury. J Neurotrauma 36(21):3051–3061
28. Mulcahey MJ et al (2013) Diagnostic accuracy of diffusion tensor imaging for pediatric cervical spinal cord injury. Spinal Cord 51(7):532–537
29. Sonoo M et al (1996) Detailed analysis of the latencies of median nerve somatosensory evoked potential components, 1: selection of the best standard parameters and the establishment of normal values. Electroencephal Clin Neurophysiol/Evoked Potentials Sect 100(4):319–331
30. Sonoo M et al (1997) Detailed analysis of the latencies of median nerve somatosensory evoked potential components, 2: analysis of subcomponents of the P13/14 and N20 potentials. Electroencephal Clin Neurophysiol/Evoked Potentials Sect 104(4):296–311
31. Tadokoro N et al (2014) Descending spinal cord evoked potentials in cervical spondylotic myelopathy: characteristic waveform changes seen at the lesion site. Clin Neurophysiol 125(1):202–207
32. Furuya S et al (2018) Highly accurate analysis of the cervical neural tract of the elderly using ZOOM DTI. Neurospine 15(2):169–174
33. Mamata H, Jolesz FA, Maier SE (2005) Apparent diffusion coefficient and fractional anisotropy in spinal cord: age and cervical spondylosis–related changes. J Magn Reson Imaging 22(1):38–43
34. Chagawa K et al (2015) Normal values of diffusion tensor magnetic resonance imaging parameters in the cervical spinal cord. Asian Spine J 9:541–547

Authors and Affiliations

Yanming Fang[1,2] · Sisi Li[3] · Jinchao Wang[1,2] · Zhenzhen Zhang[1,4] · Wen Jiang[1,5] · Chao Wang[1,6] · Yuancheng Jiang[3] · Hua Guo[3] · Xiao Han[1,2,6] · Wei Tian[1,2]

✉ Xiao Han
hanxiaomd@vip.163.com

✉ Wei Tian
tianweispine@163.com

[1] Beijing Jishuitan Hospital, Capital Medical University, Beijing, China

[2] Spine Department, Beijing Jishuitan Hospital, Capital Medical University, Beijing, China

[3] Center for Biomedical Imaging Research, Tsinghua University, Beijing, China

[4] Department of Neurological Electrophysiology, Beijing Jishuitan Hospital, Capital Medical University, Beijing, China

[5] Radiology Department, Beijing Jishuitan Hospital, Capital Medical University, Beijing, China

[6] Beijing Research Institute of Traumatology and Orthopaedics, Beijing, China